

Towards a portable setup for the on-site SERS detection of miRNAs

*Original*

Towards a portable setup for the on-site SERS detection of miRNAs / Montesi, Daniel; Bertone, Sofia; Rivolo, Paola; Geobaldo, Francesco; Giorgis, Fabrizio; Novara, Chiara; Chiado, Alessandro. - In: JOURNAL OF THE EUROPEAN OPTICAL SOCIETY. RAPID PUBLICATIONS. - ISSN 1990-2573. - ELETTRONICO. - 20:1(2024).  
[10.1051/jeos/2024028]

*Availability:*

This version is available at: 11583/2990242 since: 2024-07-02T16:13:11Z

*Publisher:*

edp sciences

*Published*

DOI:10.1051/jeos/2024028

*Terms of use:*

This article is made available under terms and conditions as specified in the corresponding bibliographic description in the repository

*Publisher copyright*

(Article begins on next page)

# Towards a portable setup for the on-site SERS detection of miRNAs

Daniel Montesi<sup>a</sup>, Sofia Bertone<sup>a</sup>, Paola Rivolo, Francesco Geobaldo, Fabrizio Giorgis, Chiara Novara<sup>\*</sup> , and Alessandro Chiadò

Politecnico di Torino, c.so Duca degli Abruzzi 24, 10129 Torino, Italy

Received 5 April 2024 / Accepted 17 May 2024

**Abstract.** The actual implementation of on-site analysis of biomarkers, such as miRNAs, depends on the availability of portable and easy-to-handle detection systems that can be used as point-of-care in real life applications. In this work, an automatized microfluidic platform combined with a portable Raman spectrometer is reported and tested for miR-214 detection by surface enhanced Raman scattering (SERS). A multi-chamber SERS-active chip, functionalized according to a previously optimized two-step hybridization assay, was automatically incubated with the analyte solution. Preliminary tests allowed to adjust the portable Raman spectrometer acquisition conditions and to compare the obtained results with those of a bench Raman microscope. Finally, miR-214 at different concentrations was analyzed through an automatic procedure, achieving a limit of detection (LOD) in the picomolar range.

**Keywords:** Surface enhanced Raman scattering, miRNA, Microfluidic setup, On-site Raman measurements.

## 1 Introduction

Surface enhanced Raman scattering (SERS) has provided excellent results in optical biosensing, since it can be used for the highly sensitive detection of molecules in complex biological samples, such as cell extracts or biofluids, taking advantage of plasmonic nanostructures [1, 2]. Indeed, the excitation of Localized Surface Plasmon Resonances of noble metal nanoparticles (NPs) generates a great enhancement of the local electric field that can be exploited to boost the Raman scattering efficiency and, thus, the sensitivity. These features are fundamental for the analysis of contaminants in food or in the environment, as well as of drugs and biomarkers in medical applications [3, 4]. In this context, the automatization and simplification of the whole analytical procedure is highly desirable as the measurements have to be performed by non-specialized users [5]. Recently, the availability of portable Raman spectrometers and the integration of plasmonic nanostructures into microfluidic devices allowed the growth of on-site sensing applications of SERS [6, 7]. However, the use of SERS biosensors in real life case studies is still sporadic due to the reduced performances out of the laboratory, to the challenges in the integration of cheap and efficient substrates into microfluidic devices and to the lack of easy-to-handle SERS detection platforms [8].

In this work, the development and optimization of a portable and automatic setup for SERS analyses is reported. The described system includes a motorized sample injection module, a support for the proper positioning of the Raman probe on the SERS-active device, the microfluidic chip and a portable Raman spectrometer, as well as a custom script that allows for syringe-pump and spectrometer control and data processing. As a proof of concept, Ag-decorated porous silicon membranes integrated into a polydimethylsiloxane (PDMS) chip were combined with the portable setup and tested for the detection of miR-214, a biomarker deregulated in several human cancers [9]. Preliminary tests were performed to adjust the acquisition conditions and to set the automatic procedure. Afterwards, the performances of the portable automatized system and of a state-of-the-art bench Raman microscope were compared by analyzing solutions containing several miR-214 concentrations, following a recently optimized two-step hybridization assay [10, 11]. The *in-chip* analysis of miR-214 and its quantification by an entirely automatized procedure was thus demonstrated.

## 2 Material and methods

The SERS nanostructures (Ag-pSi-PDMS membranes) non-integrated in the microfluidic device were used for preliminary tests and prepared as previously reported [11], while the multi-chamber SERS chip integrating the same

<sup>a</sup> These authors equally contributed to the work.

\* Corresponding author: [chiara.novara@polito.it](mailto:chiara.novara@polito.it)

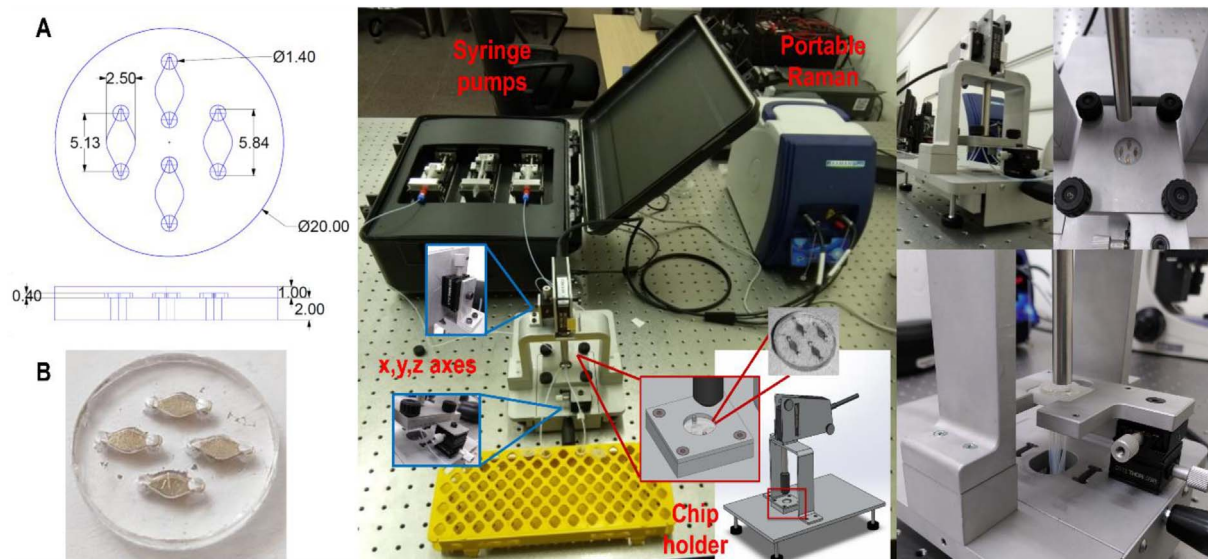


**Figure 1.** (A) Schematic top view and cross section of the microfluidic chip (dimensions in mm); (B) Representative picture of the multi-chamber microfluidic chip; (C) Experimental setup for portable SERS analyses.

nanostructures was fabricated as in [10, 12] and used for all the other tests. Compared to the previous reference works, little variations have been done to the dimensions of the microfluidic chambers and inlet/outlet ports have been moved from the top PDMS cover to the bottom layer, as detailed in Figure 1A. A picture of the microfluidic chip is reported in Figure 1B. A two-step hybridization assay exploiting DNA probes complementary to the sequence of the target miRNA was employed for miR-214 detection. Briefly, a first probe (H1, 5'-C6SH-ACTGCCTGTCT-3') is immobilized on the AgNPs surface to capture the analyte from the sample, while the second one (H2, 5'-RGX-GTGCTGTCTGT-3') binds the captured miRNA and is labelled with Rhodamine Green X (RGX) as Raman reporter, to increase the sensitivity of the assay. These steps were done as detailed in [11]. Instead, the sample incubation step was performed with the automatic injection system, by flushing 100  $\mu\text{L}$  of analyte solution continuously back and forth into the chambers of the microfluidic chip. All the SERS analyses were performed at an excitation wavelength of 532 nm in order to match the plasmon resonance of the employed SERS-active substrates [11]. An InVia Qontor Raman microscope was used as the reference bench-top instrumentation to acquire SERS maps over an area of  $110 \mu\text{m} \times 110 \mu\text{m}$  (step size =  $55 \mu\text{m}$ ) using a Leica  $10\times$  objective (NA 0.22, laser spot size  $3.5 \mu\text{m}$ ). A B&W Tek i-Raman plus spectrometer was instead included in the portable setup and used to collect SERS spectra with an optical fiber probe (laser spot size  $85 \mu\text{m}$ ) at three different points of the microfluidic chambers. SERS spectra were processed with the HyperSpec R package [13] and the Renishaw software WiRe 5.5 as described in [11]. The WiRe software was also exploited to perform cosmic rays removal and to slightly smooth the raw spectra. The limit of detection (LOD) for the calibrations measured with both setups was calculated as reported in [14] by following the linear regression method.

### 3 Results and discussion

The presented setup is composed of a portable Raman spectrometer, combined with three syringe-pumps that can be controlled to simultaneously flow the sample or washing solutions into the multi-chamber SERS chip. A special chip holder was designed to allow the microfluidic connections with the syringe-pumps and to optimize the coupling with the optical fiber probe used for the measurements with the portable spectrometer. An image of the setup is shown in Figure 1C. The injection as well as the Raman acquisition parameters can be adjusted through a custom script aimed to automatically run the microfluidics and the optical measurements, whereas only the test-tubes with sample/washing solutions must be manually changed.

Each chamber of the SERS chip integrates AgNPs of an average size of 30 nm that form a homogeneous and densely packed layer on the porous silicon membrane, providing numerous hot-spots for an efficient SERS detection [11].

Preliminary tests were performed to compare the performances of the portable spectrometer with those of the bench Raman microscope. To this aim, solutions with different concentration of Rhodamine 6G, a typical SERS reporter, were incubated on the surface of non-integrated SERS-active nanostructures and measured with the two instruments. As reported in Figure 2A, similar spectra were obtained with the two spectrometers. Indeed, by adjusting the exposure time and the excitation laser power, the vibrational fingerprint of Rhodamine 6G (main peaks at  $612, 774, 1364, 1509, 1573$  and  $1648 \text{ cm}^{-1}$  [15]) was detected with comparable intensity and signal-to-noise ratio for the same concentration of the analyte. Then, acquisition conditions were further optimized by analyzing the SERS chip functionalized by the two-step assay with the portable setup. In particular, since proper focusing of solid SERS substrates is crucial, the chip holder was designed to control the distance of the sample vs. the optical fiber probe, which

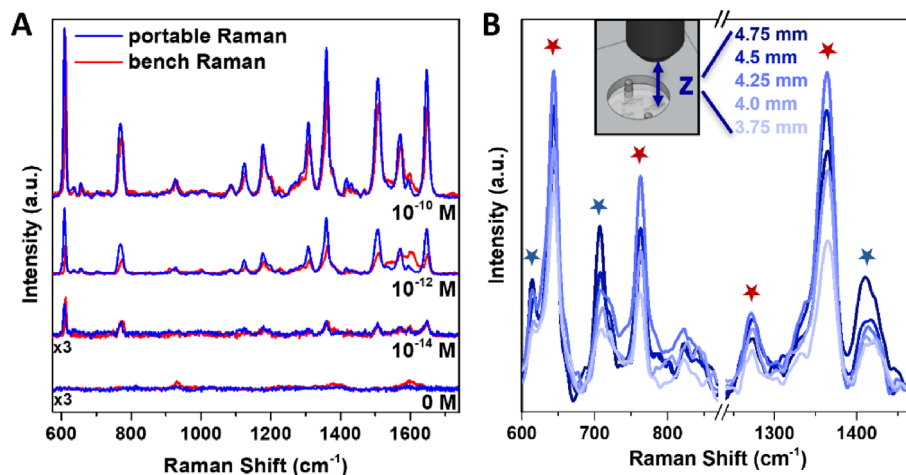


**Figure 2.** (A) SERS spectra of Rhodamine 6G ethanolic solutions at different concentration ( $10^{-10}$ – $10^{-14}$  M) incubated on the non-integrated SERS-active nanostructures measured with a bench Raman microscope (red curves – acquisition time 60 s, laser power 0.02 mW) or with the portable Raman spectrometer (blue curves – acquisition time 150 s, laser power 0.6 mW); (B) Optimization of the chip-optical fiber probe distance ( $z = 0$  corresponds to the microfluidic chip surface). SERS spectra (acquisition time 30 s, laser power 3.8 mW) of the microfluidic chip functionalized with the H1 probe, incubated with the target miR-214 at 10 nM concentration and then with 1  $\mu$ M RGX-labelled H2 probe (red stars: RGX bands; blue stars: PDMS bands).

is used to excite the plasmonic substrate and to collect the scattered beam. As a result, the SERS signal can be maximized to reach satisfying results without a bulky microscope. Figure 2B provides a clear demonstration of this feature: in this example, the microfluidic chip, functionalized with the H1 probe, was incubated with the target miR-214 and then with the RGX-labelled H2 probe. Afterwards, the Raman measurements were performed by moving in  $z$  the optical fiber probe. By looking at the vibrational bands of the Raman reporter (highlighted by red stars), it is clear that the maximum of the RGX signal intensity is reached when the probe is located 4.25 mm far from the surface of the chip. In such configuration, the laser beam is suitably focused on the surface of the plasmonic nanostructures integrated in the microfluidic chip, thus maximizing the intensity of the SERS signal and increasing the sensitivity of the bioassay. At the same time, such optimal distance reduces the unwanted background due to PDMS vibrational pattern (blue stars), one of the main components of the microfluidic device.

After these optimizations, the microfluidic chip combined with the portable setup was tested for miR-214 detection and the results compared with those of the bench Raman microscope. Therefore, the AgNPs were functionalized to graft the H1 probe, and then the chip was connected to the microfluidic setup. A volume of 100  $\mu$ L of miR-214 solution in the 10–0.1 nM range was dynamically incubated in the microfluidic chips, followed by the incubation of the H2-RGX probe at 1  $\mu$ M concentration. Afterwards, the device was analyzed by means of the bench and portable Raman spectrometers. The results are displayed in Figure 3A and 3B. In both cases the Raman signal of the vibrational bands of RGX at 635 and 1364  $\text{cm}^{-1}$  are clearly detectable down to the lowest analyzed concentration, namely 0.1 nM. Moreover, a quantitative comparison of the performances of the bench and portable setups was

accomplished by calculating the LOD of miR-214. To this aim, deconvolution procedures through Lorentzian curves were carried out in order to calculate the areas under the isolated peak at 635  $\text{cm}^{-1}$ , which were then plotted as a function of the miRNA concentration. By performing a linear regression of such calibration curves, LODs equal to 0.27 nM and 0.21 nM were obtained concerning the measurements with the bench (Figure 3C) or the portable (Figure 3D) spectrometers, respectively. Such result demonstrates that both setups can achieve the same level of sensitivity, within a picomolar regime. This outcome is probably due to the high sensitivity that can be reached in the detection of miRNAs by using the optimized two-step bioassay combined with the integration of the SERS substrates in microfluidic chips. Thus, even with a portable Raman spectrometer a similar sensitivity can be attained at a lower cost, compared to the bench apparatus.

Finally, the automatic spectral analysis was also tested. Indeed, a calibration curve similar to the one reported in Figure 3 can be obtained by analyzing the spectra measured through the portable apparatus by means of custom scripts able to automatically remove the background and calculate the area under the vibrational band of interest. More in detail, 6th-degree polynomial curves were employed to subtract the baseline from the spectra, mostly due to the intrinsic fluorescence of the Raman reporter. An example of such automatic baseline subtraction procedure is reported in Figure 4A. The areas under the RGX peak at 635  $\text{cm}^{-1}$  were calculated as the sum of the intensity counts in a specific Raman shift range (615–655  $\text{cm}^{-1}$ ) and afterwards plotted as a function of the miRNA concentration. The corresponding calibration curve is reported in Figure 4B, which can be exploited to quantify miR-214 in a sample analyzed by means of the portable setup. By performing a linear regression of this calibration curve, a LOD equal to 0.44 nM was obtained. Such value is almost double than

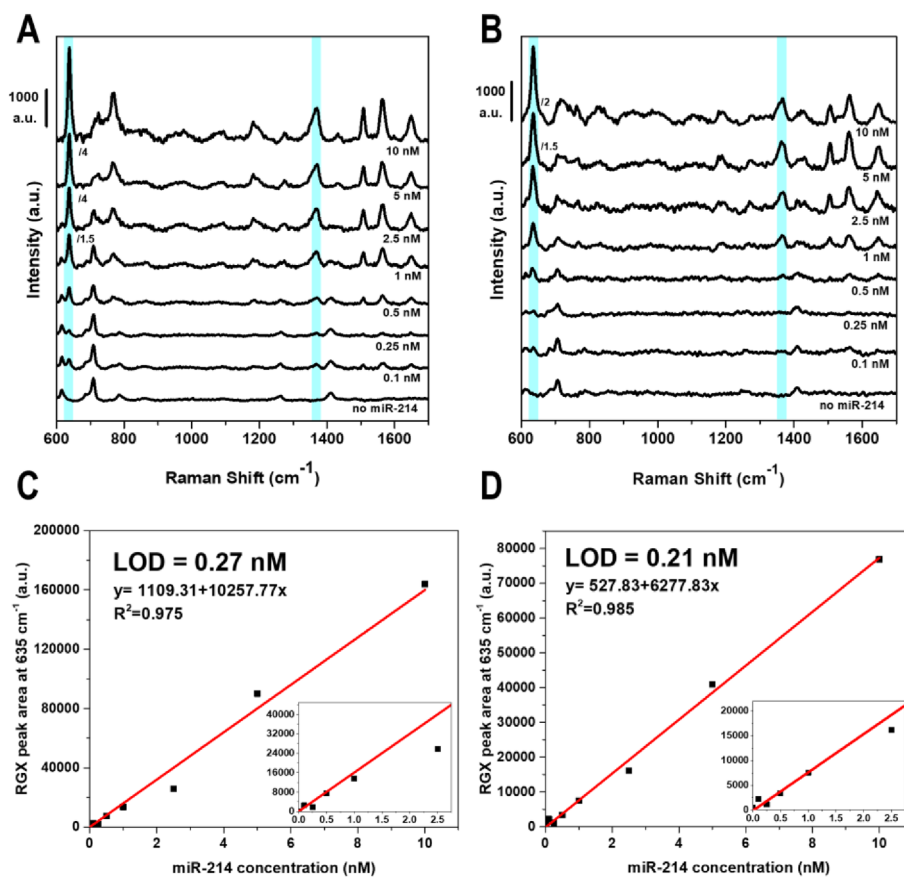


**Figure 3.** SERS spectra obtained by measuring the plasmonic nanostructures integrated in microfluidic chips and functionalized according to the two-step assay for the detection of miR-214 (0.1–10 nM), by means of (A) the bench (acquisition time 60 s, laser power 0.2 mW) or (B) the portable (acquisition time 10 s, laser power 3.8 mW) Raman spectrometers. The light blue bars highlight the main vibrational bands of RGX reporter. Linear regression of the calibration curves relative to the in-chip SERS analysis of miR-214; (C) obtained with the bench spectrometer; (D) obtained with the portable setup; the insets highlight the trend at the lowest miRNA concentrations.

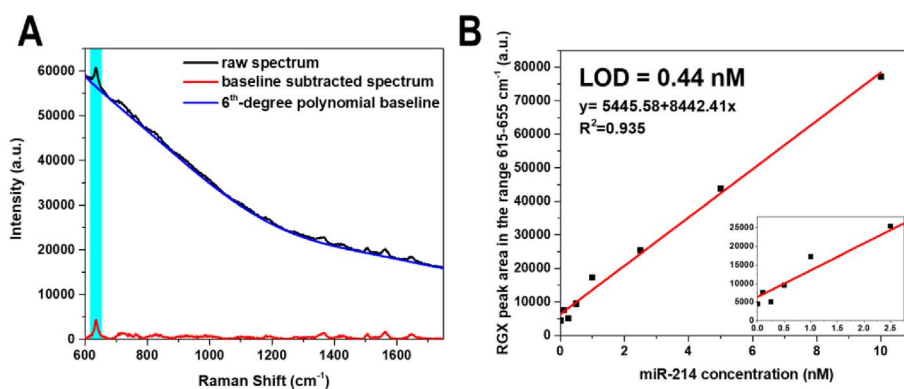


**Figure 4.** (A) Example of automatic baseline subtraction concerning the analysis of 10 nM miR-214 (main vibrational band of RGX at  $635\text{ cm}^{-1}$ , light blue bar); (B) linear regression of the calibration curve obtained by the automatic analysis of the spectra measured with the portable Raman spectrometer. The inset highlights the trend at the lowest miRNA concentrations.

the one previously calculated by manually analyzed spectra. This is probably explained by the rough method employed to automatically process the spectral data. Indeed, the area of the peak of interest calculated as the sum of counts in a

predetermined Raman shift interval may include the contribution of overlapped vibrational bands, especially at low target concentrations. Such approach yields a possible overestimation of the detection limit. Nevertheless, it should be

noted that the simplified and automatic procedure developed has the advantage to be suitable for on-site analyses, while rigorous deconvolution processes are extremely difficult to automate with reliability in this kind of applications.

## 4 Conclusions

A portable and automated setup for the detection of miRNAs by SERS analysis was developed and tested for the detection of miR-214. After a fine adjustment of the acquisition conditions, similar spectra, in terms of intensity and signal-to-noise ratio, were obtained with the portable spectrometer compared to a bench Raman microscope. The performances of the portable setup were checked also by measuring different concentrations of miR-214 with both the bench and the portable Raman spectrometers. Comparable LODs were attained by analysing the spectra acquired with both setups. Moreover, the combination of the SERS-chip with the liquid handling system and the portable Raman spectrometer through custom scripts, allowed to automate both the measures and the analyses, showing a high potential for on-site analyses of miRNAs with a sensitivity at picomolar concentration.

### Funding

This publication is part of the project NODES which has received funding from the MUR – M4C2 1.5 of PNRR with grant agreement no. ECS00000036.

Italian Ministry of University and Research (MUR) is acknowledged for funding through the project PRIN 2022 SEMPER (Grant Nr. 20227ZXT4Z).

### Conflicts of interest

The authors declare that they have no competing interests to report.

### Data availability statement

Data will be made available on request.

### Author contribution statement

Conceptualization: AC, CN; Formal analysis: CN, AC and DM; Investigation: DM, SB, AC, PR and CN; Methodology: SB, AC and CN; Supervision: AC, CN, FrG and FaG; Visualization: CN, DM and AC; Writing– original draft: AC; Writing – review & editing: AC, CN, PR, DM, SB, FrG and FaG.

### References

1 Langer J., et al. (2020) Present and future of surface-enhanced Raman scattering, *ACS Nano* **14**, 28–117.

- 2 Fan M., Andrade G.F.S., Brolo A.G. (2020) A review on recent advances in the applications of surface-enhanced Raman scattering in analytical chemistry, *Anal. Chim. Acta* **1097**, 1–29.
- 3 Perumal J., Wang Y., Attia A.B.E., Dinish U.S., Olivo M. (2021) Towards a point-of-care SERS sensor for biomedical and agri-food analysis applications: A review of recent advancements, *Nanoscale* **13**, 553–580.
- 4 Liao W., Lu X. (2016) Determination of chemical hazards in foods using surface-enhanced Raman spectroscopy coupled with advanced separation techniques, *Trends Food Sci. Technol.* **54**, 103–113.
- 5 Jahn I., Zukovskaja O., Zheng X.-S., Weber K., Bocklitz T., Cialla-May D., Popp J. (2017) Surface enhanced Raman spectroscopy and microfluidic platforms: Challenges, solutions and potential applications, *Analyst* **142**, 1022–1047.
- 6 Guo J., Liu Y., Ju H., Lu G. (2022) From lab to field: Surface-enhanced Raman scattering-based sensing strategies for on-site analysis, *TrAC – Trends Anal. Chem.* **146**, 116488.
- 7 Sun J., Gong L., Wang W., Gong Z., Wang D., Fan M. (2020) Surface-enhanced Raman spectroscopy for on-site analysis: A review of recent developments, *Luminescence* **35**, 808–820.
- 8 Guo J., Zeng F., Guo J., Ma X. (2020) Preparation and application of microfluidic SERS substrate: Challenges and future perspectives, *J. Mater. Sci. Technol.* **37**, 96–103.
- 9 Penna E., Orso F., Taverna D. (2015) miR-214 as a key hub that controls cancer networks: Small player, multiple functions, *J. Investig. Dermatol.* **135**, 960–969.
- 10 Novara C., Chiadò A., Paccotti N., Catuogno S., Esposito C. L., Condorelli G., De Franciscis V., Geobaldo F., Rivolo P., Giorgis F. (2017) SERS-active metal-dielectric nanostructures integrated in microfluidic devices for label-free quantitative detection of miRNA, *Faraday Discuss.* **205**, 271–289.
- 11 Novara C., Montesi D., Bertone S., Paccotti N., Geobaldo F., Channab M., Angelini A., Rivolo P., Giorgis F., Chiadò A. (2023) Role of probe design and bioassay configuration in surface enhanced Raman scattering based biosensors for miRNA detection, *J. Colloid Interface Sci.* **649**, 750–760.
- 12 Novara C., Lamberti A., Chiadò A., Virga A., Rivolo P., Geobaldo F., Giorgis F. (2016) Surface-enhanced Raman spectroscopy on porous silicon membranes decorated with Ag nanoparticles integrated in elastomeric microfluidic chips, *RSC Adv.* **6**, 21865–21870.
- 13 Beleites C., Sergio V. (2015) *hyperSpec: A package to handle hyperspectral data sets in R.* <http://hyperspec.r-forge.r-project.org>.
- 14 Shrivastava A., Gupta V. (2011) Methods for the determination of limit of detection and limit of quantitation of the analytical methods, *Chronicles Young Sci.* **2**, 21–25.
- 15 Virga A., Rivolo P., Frascella F., Angelini A., Descrovi E., Geobaldo F., Giorgis F. (2013) Silver nanoparticles on porous silicon: Approaching single molecule detection in resonant SERS regime, *J. Phys. Chem. C* **117**, 20139–20145.